Origin of carbonatites of the Matcha alkaline pluton from Turkestan-Alai ridge, Kyrgyz Southern Tien Shan

V V Vrublevskii

Department of Geology and Geography, Tomsk State University, Lenin Avenue 36, Tomsk, 634050, Russia

E-mail: vasvr@yandex.ru

Abstract. Postorogenic alkaline intrusions in the Turkestan-Alai segment of the Southern Tien Shan coexist with dikes and veins of carbonatites dated at ~220 Ma. They are primarily composed of calcite and dolomite (60–85 %), as well as sodic amphibole, phlogopite, clinopyroxene, microcline, albite, apatite, and magnetite, with accessory niobate, ilmenite, Nb-rutile, titanite, zircon, baddeleyite, monazite-(Ce), barite, and sulfides. The rocks share mineralogical and geochemical similarity with carbonatites that originated by liquid immiscibility at high temperatures above 500°C. Silicate and salt-carbonate melts are derived from sources with mainly negative bulk $\varepsilon Nd(t)$ ~ from –11 to 0 and high initial $^{87}Sr/^{86}Sr$ ratios (~ 0.7061-0.7095) which may be due to mixing of PREMA and EM-type mantle material. Pb isotopic ratios in accessory pyrrhotite ($^{206}Pb/^{204}Pb$ = 18.38; $^{207}Pb/^{204}Pb$ = 15.64; $^{208}Pb/^{204}Pb$ = 38.41) exhibit an EM 2 trend. The intrusions bear signatures of significant crustal contamination as a result of magma genesis by syntexis and hybridism. Concordant isotope composition changes of $\delta^{13}C$ (–6.5 to −1.9 ‰), $\delta^{18}O$ (9.2-23 ‰), δD (–58 to –41 ‰), and $\delta^{34}S$ (12.6-12.8 ‰) in minerals and rocks indicate inputs of crustal material at the stage of melting and effect of hot fluids released during dehydration of metamorphosed oceanic basalts or sediments. The observed HFSE patterns of the oldest alkaline gabbro may be due to interaction of the primary mafic magma with IAB-type material. The isotope similarity of alkaline rocks with spatially proximal basalts of the Tarim large igneous province does not contradict the evolution of the Turkestan-Alai Triassic magmatism as the «last echo» of the Tarim mantle plume.

1. Introduction

Formation of carbonatites is usually associated with either fractional crystallization of CO_2-saturated alkali-silicate magmas, or intrusion and crystallization of alkali-dolomite magma from independent mantle sources [1–3]. Bear signature of crustal contamination of magmatic derivatives is recorded in volcano-plutonic complexes in Phanerozoic orogenic belts [4-7].

In Kyrgyz Southern Tien Shan, dikes and veins of carbonatites Ar–Ar dated at ~220 Ma complete forming postorogenic Late Triassic alkaline intrusions of the Turkestan-Alai Ridge. Plutons are composed by essexites, foidolites, nepheline and alkaline syenites [8–10]. The most abundant carbonatite veins are concentrated in the Delbek valley that cuts the North-Eastern contact of Matcha pluton (~ 30 km^2), they occur as up to 100–400 m long injection zones together with syenite offshoots among fenitized schists. Some veins are small (to n × 1 m) and often form branching systems and thick lenses. Carbonatites have massive or banded, schlieric-taxitic structures. Predominant carbonates (calcite and dolomite, 60–85 %) commonly occur as fine- to medium-grained aggregates, often with round porphyritic crystals that enclose particles of other typical phases (10–35 %): alkaline amphiboles, clinopyroxenes and feldspar, micas, apatite and magnetite. Accessory sulfides (pyrrhotite, pyrite, etc.), pyrochlore, monazite, titanite, zircon, baddeleyite, thorite, ilmenite, ilmenorutile, rutile, barite occur sporadically as scarce microcrysts or euhedral grains (~ 0.01–1 mm) in a silicate-carbonate matrix [11–12]. Observed signs of deformation with twinning bends in carbonates, along with kink-bands in mica flakes and banded structures as evidence of possible plastic flow. Geochemical characteristics suggest mantle-crustal matter source and liquid immiscibility origin of carbonatites.

2. Chemical composition of alkaline rocks and carbonatites

For silicate rocks of typical alkaline plutons (Matcha and Zardalek ones) from gabbro to foydolites and syenites, it is typical to see increase in concentrations of SiO_2 ~ from 40 to 66 wt. %, Al_2O_3 ~ from 12 to 29 wt. %, ($Na_2O + K_2O$) ~ from 2.3 to 19 wt. %. At the same time following concentrations decrease: MgO ~ from 11 to 0.3, CaO ~ from 20 to 2 and Fe_2O_3 ~ from 14 to 2 wt. % (table 1).

Table 1. Representative chemical composition of igneous alkaline rocks and carbonatites from Turkestan-Alai ridge[a].

Massif	Matcha					Zardalek				
Rock[b]	1[c]	2[c]	3[c]	4	5	6	7	8	9	10
SiO_2, wt. %	49.65	52.06	62.51	1.23	1.03	3.28	13.55	51.82	42.47	53.39
TiO_2	1.00	0.68	0.12	0.04	0.02	0.03	0.18	0.67	0.40	0.18
Al_2O_3	16.15	20.25	16.64	0.05	0.30	0.60	2.95	11.97	28.94	25.99
Fe_2O_3	10.99	7.70	5.10	1.97	1.77	1.53	1.01	8.51	3.91	1.82
MnO	–[d]	0.13	0.09	0.13	0.18	0.21	0.12	0.13	0.12	0.06
MgO	2.64	0.21	0.47	0.05	2.16	13.90	7.87	10.77	0.89	1.51
CaO	8.78	4.51	2.72	53.98	53.39	36.17	39.64	8.39	3.39	1.38
Na_2O	5.26	7.60	6.80	0.30	0.08	0.34	0.60	1.62	8.50	4.22
K_2O	4.86	4.92	6.22	0.20	0.08	0.32	1.85	1.37	7.51	9.23
P_2O_5	0.06	0.08	0.03	0.80	3.22	3.77	2.34	0.30	0.16	0.03
LOI	1.10	3.08	0.22	40.99	37.01	39.23	29.28	4.06	3.33	1.92
Total	100.49	101.22	100.92	99.74	99.24	99.38	99.39	99.61	99.62	99.73
Cr, ppm	–	9.5	9.8	2.7	7	1.5	3.7	596	5.2	3.5
Ni	–	1.6	2.6	13	25	18	19	63	3.1	2.4
V	–	9	21	6	2.2	10	18	164	40	13
Co	–	3.5	4.5	1.7	5	3.1	3.4	32	6	2.5
Sc	–	0.6	1.3	1.6	1.2	0.8	1.3	26	1.1	0.34
Pb	–	18	39	53	17	–	–	7.5	51	108
Cs	–	2	5.6	1.7	0.3	0.1	17	1.4	27	25
Rb	90	255	226	42	9.2	10	211	41	339	314
Ba	3100	715	854	1985	616	270	554	469	1190	1820
Sr	740	430	315	4056	2692	1426	2035	342	1011	1396
Y	24	14	7.5	182	40	8.5	32	13	15	3
Zr	120	124	249	25	1.8	1.8	6.6	84	110	64
Hf	2.7	3.8	6.7	0.3	0.1	0.12	0.28	2.2	1.6	0.92
Nb	24	51	44	12	9.4	11	14	9.6	12	20
Ta	1.5	2.3	2.1	0.8	0.9	0.93	1	3	0.83	1.2
Th	6.5	4	6.6	0.3	0.9	2.3	0.61	5.1	19	56
U	2.6	2.2	2.9	0.2	1.6	8.7	0.96	2.5	10	28
ΣREE	320.7	115.7	63.1	707.1	205	56.6	146.3	89.2	178.8	147.3

[a] The ICP-MS and XRF analyses were carried out at the National Research Tomsk State University (Tomsk), at the Institute of Geology and Mineralogy SB RAS (Novosibirsk) and the Institute of Mineralogy, Geochemistry and Crystal Chemistry of Rare Elements RAS (Moscow) on an Agilent 7500cx, Elan-6100 DRC, Finnigan MAT spectrometers and a Thermo Scientific ARL-9900XP instrument under standard operating conditions.

[b] 1, 8 = subalkaline and alkaline gabbro; 2, 10 = nepheline syenite; 3 = alkaline syenite; 9, 10 = foidolite; 4–7
= carbonatites: REE-enriched variety (4), REE-depleted variety (5, 6), melanocratic variety (7).
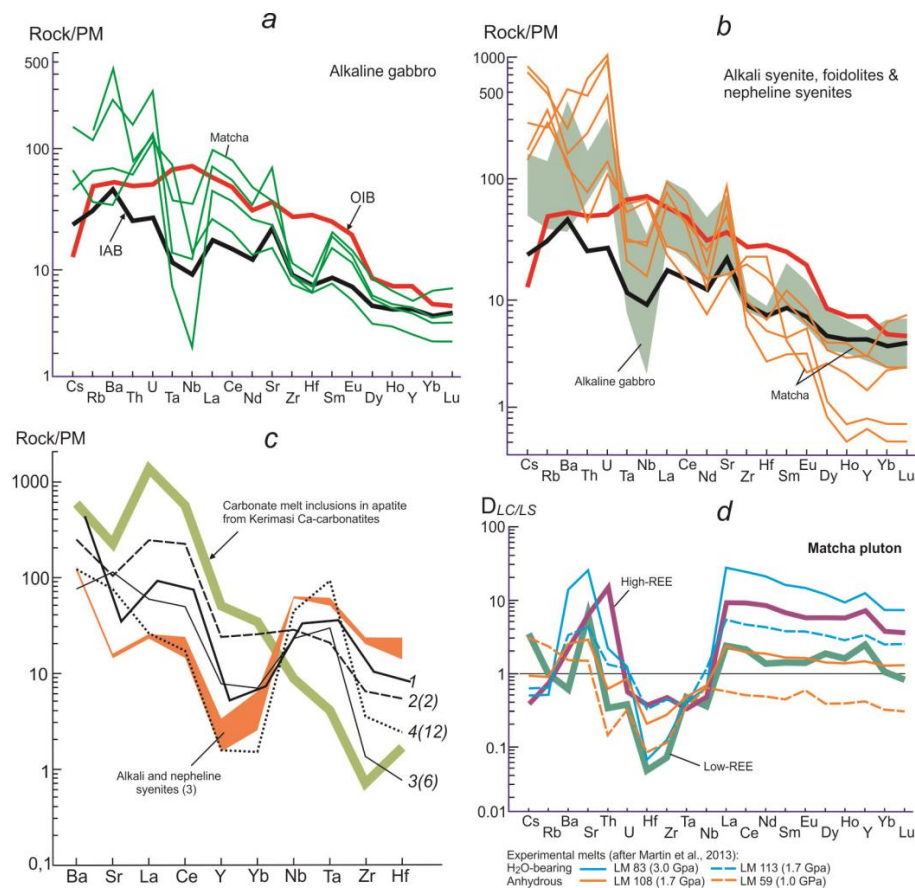[c] after Nenahov, 2002 [9].
[d] (–) is not detected.

Figure 1. Primitive mantle-normalized [13] multi-element diagrams (*a–c*) of the Matcha alkaline rocks and carbonatites and experimental carbonate-silicate melt partition coefficients ($D_{LC/LS}$) of trace elements [15] and their ratios (*d*) for the Matcha carbonatites and nepheline syenite. In panels (*a–b*) shows OIB [13] and IAB [14] average compositions. In panel (*c*), trace elements are ordered according to their decreasing experimental partition coefficients between immiscible silicate-carbonate liquids: *1* = essexite; *2* = high-REE carbonatites; *3* = low-REE carbonatites (6); *4* = low-REE carbonatites (12); numerals in braces show number of analyses. In panel (*d*), lines «High-REE» and «Low-REE» refer to trace element ratios of high-REE carbonatites, average for two samples and low-REE carbonatites, average over six samples, with average nepheline syenite (two samples).

Nature of alkalinity (up to 2–9 wt. % $_2O$; 0.8–2.2 K_2O/Na_2O) suggests that the rocks are derivatives of shoshonite series of active continental margins (ACM). In more differentiated varieties, amount of siderophile elements (4–596 Cr, 2–63 Ni, 1.3–227 V, 3–38 Co, 0.3–26 Sc, ppm) decreases, enrichment in Cs, Rb, Ba, Th, U occurs at OIB level and higher, and less in Nb, Ta and LREE. Sr content reaches ~ 1400-1800 ppm, which could be caused by crust contamination of melts. Distribution of rare earth elements (average REE ~ 200 ppm; La/Yb$_N$ 10-17) and other trace elements in gabbro is similar to

island arc basalt (IAB) compositions and partially to oceanic island basalt ones (OIB) (figure 1a, b). In later foidolites and syenites, REE concentrations decrease on average down to 140 ppm at wide ranges of La/Yb_N ~ 2-150. It might be due to dilution of a melt by REE-depleted crustal material.

Carbonatites contain ~ 34–55 wt. % CaO, ~ 0.1–17 wt. % MgO, ~ 0.3–19 wt. % SiO_2, ~ 0.3–5.6 wt. % P_2O_5, ~ 0.8–3.5 wt. % Fe_2O_3, ~ 0.1–3 wt. % ($Na_2O + K_2O$). Content of typomorphic trace elements reaches up to ~ 1500–4000 ppm Sr, ~ 500–2400 ppm Ba, ~ 20–140 ppm Zr, ~ 10–70 ppm Nb, ~ 250–1030 ppm (REE + Y). Sr/Ba ratios, which are >1 (from 2 to 17), and Th/U ≈ 0.1 to 53 indicate relatively high-temperature settings for formation and possible heterogeneity of the rocks. There are three groups with REE contents: up to 700-1000, 150-270, 23-106 ppm. At the same time, distribution of La, Ce, Yb and Y, as well as Sr, Nb, Ta, Zr, and Hf in these rocks is complimentary in relation to multistage spectrum of alkaline rocks (figure 1c, d), which is noted in experimental systems with silicate-carbonate immiscibility and in some natural melts [15-18]. Comparing to syenites, carbonatites are enriched in REE and Sr, but depleted in Nb, Ta, Zr and Hf.

3. Isotope systematics of alkaline intrusions

The initial $^{87}Sr/^{86}Sr$ and $^{143}Nd/^{144}Nd$ ratios in alkaline rocks vary from 0.70601 to 0.70915 and 0.512035 to 0.512363, respectively (table 2). The carbonatite samples have similar Nd isotope ratios (0.511803–0.512143, $\varepsilon_{Nd}(t)$ from −10.8 to −4.1) but contain more radiogenic strontium ^{87}Sr (0.70705–0.70947, 40 to 74 $\varepsilon_{Sr}(t)$). This distribution may record the evolution of alkaline magmatism in the case of juvenile PREMA–type material mixed with that of both enriched lithospheric mantle (EM) and upper crust. Similar isotope parameters with +0.2 to−10.1 ε_{Nd} and 8–67 ε_{Sr} are observed in Mesozoic (about 120–220 Ma) alkaline rocks and carbonatites located within orogenic areas of Southern Mongolia, Gornyi Altai and Western Transbaikalia in the Central Asian and Qinling (Central China) belts (figure 2a).

Table 2. Sr–Nd isotopic composition for the alkaline rocks and carbonatites of the Turkestan–Alai[a].

Sample	Massif	Rock, mineral	$^{143}Nd/^{144}Nd$	± 2σ	$^{143}Nd/^{144}Nd(t)$	$\varepsilon_{Nd}(t)$	$^{87}Sr/^{86}Sr$	± 2σ	$^{87}Sr/^{86}Sr(t)$	$\varepsilon_{Sr}(t)$
1	Z[b]	Alkaline gabbro	0.512537	12	0.512363	0.16	0.70855	18	0.70833	57.99
3		Alkaline gabbro	0.512208	14	0.512035	−6.25	0.70706	17	0.70691	37.87
5		Foidolite	0.512277	8	0.512198	−3.06	0.70740	15	0.70669	34.73
9		Foidolite	0.512239	13	0.512183	−3.36	0.70824	16	0.70724	42.63
10		Nepheline syenite	0.512507	19	0.512340	−0.29	0.70705	18	0.70601	25.11
XXX	M[b]	Nepheline syenite	0.512318	8	0.512132	−4.36	0.71190	19	0.70915	69.71
1-8-2		Glimmerite	0.512148	6	0.511971	−7.50	0.70956	21	0.70872	63.60
1084		Carbonatite	0.512092	4	0.511932	−8.26	0.70779	11	0.70772	49.34
2-3		Carbonatite	0.512272	20	0.512108	−4.82	0.70788	16	0.70783	50.96
1085		Carbonatite	0.512332	14	0.512143	−4.14	0.70882	18	0.70876	64.10
12-5		Carbonatite	0.511966	14	0.511803	−10.8	0.71008	14	0.70947	74.31
1086		Carbonatite, Ap[c]					0.70749	9	0.707484	46.05
1080/2		Carbonatite, Amp[c]					0.70825	9	0.707045	39.82

[a] Sr–Nd isotopic composition was analyzed by the standard techniques on a Finnigan MAT 262 and an MI 1201–T mass spectrometers in the static mode at the Geological Institute of the Kola Science Center RAS (Apatity).
[b] *Z* – Zardalek intrusion, *M* – Matcha intrusion.
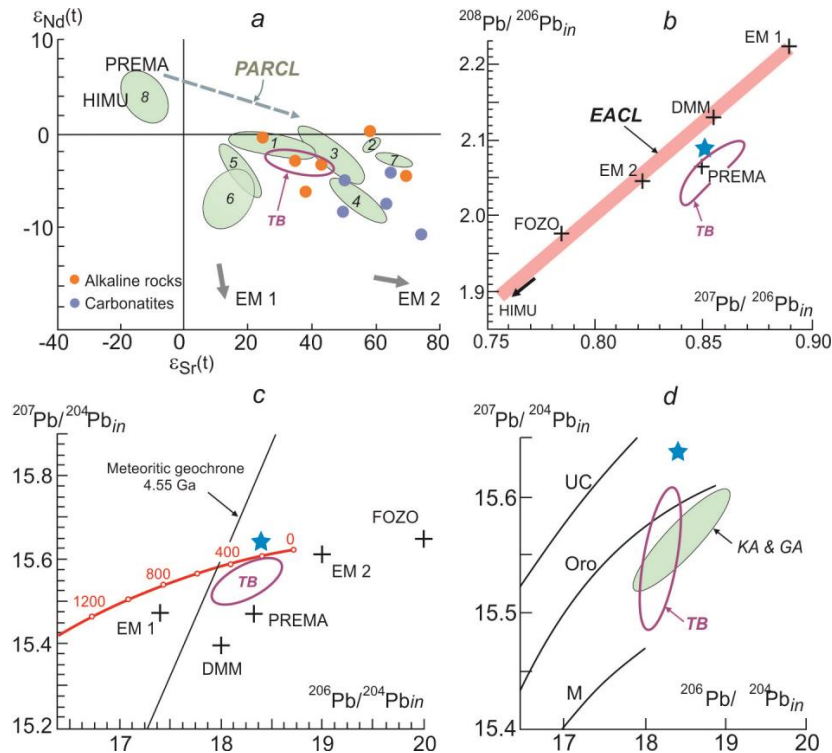[c] *Ap* = apatite, *Amp* = amphibole.

Petrology

IOP Conf. Series: Earth and Environmental Science **110** (2017) 012023

IOP Publishing

doi:10.1088/1755-1315/110/1/012023

Figure 2. $\varepsilon_{Nd}(t)$ vs. $\varepsilon_{Sr}(t)$ plot (*a*) and Pb isotope composition (*b–d*) of pyrrhotite (blue star) for the Turkestan-Alai alkaline rocks and carbonatites, and some other carbonatite-alkaline complexes from the western Central Asian Orogenic Belt and Precambrian cratons. In panel (*a*), fields in greenish show predominant compositions of Mushugai-Khuduk and Bayan-Khushu (*1*), Lugin-Gol (*2*), Beltsin-Gol and Overmaraat-Gol (*3*) complexes in Mongolia; Darai-Pioz (*4*) complex in Tajikistan; Arshan, Khalyuta, Oshurkovo (*5*) complexes in Western Transbaikalia; Huayangchuan, Yuantou, Qinlongtou, Dashigou, and Shijiawan (*6*) complexes in Central China, lamproites in Gornyi Altai (*7*) and carbonatites from the Siberian, European and Northern American cratons (*8*) [19–23]. Contour *TB* is isotopic range of basalts from the Tarim large igneous province [24–26]; Western CAOB Paleozoic alkaline rocks and carbonatites line (*PARCL*) is according to (Doroshkevich et al., 2012; Vrublevskii et al., 2012; Vrublevskii, 2015) [5–7]; PREMA, HIMU, EM1 and EM2 mantle reservoirs are according to (Zindler and Hart, 1986; Stracke et al., 2005) [27, 28]. In panel (*b–d*), the elements of plumbotectonics, lead isotope evolution and mantle components of PREMA (Prevalent Mantle), FOZO (Focus Zone), HIMU (High-µ), DMM (Depleted MORB Mantle), EM1 (Enriched Mantle 1) and EM2 (Enriched Mantle) reservoirs are according to (Stacey and Kramers, 1975; Zartman and Doe, 1981; Zindler and Hart, 1986; Hart et al., 1992; Stracke et al., 2005; Armienti and Gasperini, 2007) [27–32]; East African Carbonatite Line (*EACL*) is after (Bell and Tilton; 2001) [33]; area *KA&GA* represents alkaline rocks and carbonatites of the Kuznetsk Alatau and Gornyi Altai in the western CAOB [34]. Abbreviations in panel (*d*) stand for UC = upper crust, Oro = Orogenic, M = Mantle.

Initial Pb isotope ratios in pyrrhotite from carbonatites ($^{206}Pb/^{204}Pb$ 18.38; $^{207}Pb/^{204}Pb$ 15.64; $^{208}Pb/^{204}Pb$ 38.41) indicate interaction with EM2 source (figure 2b, c). Enrichment of the mineral in radiogenic ^{207}Pb and ^{206}Pb also allows us to assume participation of upper crustal material in petrogenesis that is typical for orogenic areas (figure 2d). The isotopic composition of lead in pyrrhotite was measured by the standard techniques on a Thermo Scientific Neptune MC-ICP-MS

mass spectrometer at the Institute of Geology of Mineral Deposits, Petrography, Mineralogy and Geochemistry RAS (Moscow).

Values $\delta^{13}C$ (from −6.5 to −1.9 ‰) and $\delta^{18}O$ (18–23 ‰) in carbonates correlate directly (table 3, figure 3a); such correlation is often noticed when mixing mantle-derived and sedimentary CO_2 [39, 40]. It looks like crustal contamination occurred at the melting stage, which caused simultaneous enrichment in ^{18}O silicates ($\delta^{18}O$ 11.9–16.5 ‰), apatite ($\delta^{18}O$ 17.2 ‰) and magnetite ($\delta^{18}O$ 11.9–13.5 ‰). Variations of δD in water-bearing silicates (from −41 to −58 ‰; table 3, figure 3b) coincide with range from −40 to −90 ‰ in amphiboles and micas from mantle rocks [38]. However, level of enrichment in ^{18}O corresponds better to metamorphic waters. Studied pyrrhotine is enriched in $\delta^{34}S$ = 12.6–12.8 ‰ comparing to meteorite standard $\delta^{34}S_{CDT} \sim 0$ ‰, which is possible when mixing of juvenile mantle-derived and sedimentary sulfur. $\delta^{34}S$ values were determined at the isotope laboratory of the Geological Institute RAS, Moscow on a MI 1201−V mass spectrometer.

Table 3. Isotopic composition of O, C and H for the Turkestan−Alai alkaline rocks and carbonatites[a].

Massif	Rock	Sample	Material	$\delta^{13}C$, ‰	$\delta^{18}O$, ‰	δD, ‰	T, °C[d]
M [b]	Carbonatite	1086	Cb[c]	−3.9	20.7		
			Ap		17.2		403, 508[e]
	Carbonatite	1085	Cb	−4.4	18.0		
			Lpm		11.9	−58	
	Carbonatite	1084	Cb	−6.5	18.6		
	Carbonatite	12-5	Cb	−4.0	19.8		
	Carbonatite	12-1	Cb	−3.0	21.4		
	Carbonatite	1080	Cb	−2.7	22.1		
			Phl		16.4		
	Carbonatite	1080/1	Cb	−2.3	23.0		
			Mag		13.5		504
	Carbonatite	1080/2	Cb	−3.5	21.2		
			Phl		14.7	−57	
			Amp		16.5	−41	
	Carbonatite	1081	Cb	−1.9	21.8		
			Phl		16.1		
			Mag		11.9		488
Z [b]	Alkaline gabbro	1	WR		9.8		
	Alkaline gabbro	3	WR		9.2		
	Foidolite	5	WR		12.0		
	Foidolite	9	WR		12.4		
	Nepheline syenite	10	WR		9.4		

[a] The $\delta^{13}C_{V-PDB}$, $\delta^{18}O_{V-SMOW}$ and δD_{V-SMOW} values were determined at the isotope laboratories of the Geological Institute RAS (Moscow) and the Geological Institute SB RAS (Ulan-Ude) on a MI 1201−V, GD−150, Delta V Advantage and a Finnigan MAT 253 mass spectrometers.

[b] M – Matcha intrusion, Z – Zardalek intrusion.

[c] Cb = carbonate, Ap = apatite, Amp = amphibole, Phl = phlogopite, Lpm = lepidomelane, Mag = magnetite, Cc = calcite, WR = whole rock.

[d] Isotopic temperatures were calculated from the relation: 1000 lnα (calcite–magnetite) = 5.74 × $10^6/T^2$, after Clayton and Kieffer, 1991 [43], 1000 lnα (calcite–apatite) = 1.6 × $10^6/T^2$, after Fortier, Luttge, 1995 [44].

[e] calculated as in Alberti et al., 1999 [45].

4. Discussion
4.1. Conditions of the petrogenesis
Important geochemical characteristics of studied rocks are their general depletion in REE and high values of $^{87}Sr/^{86}Sr(t)$ and $\delta^{18}O$. The patterns we have found out let us assume that evolution of parent

alkali-mafic magma in the lithospheric mantle was concurrent with melting and assimilation of crustal rocks (syntexis), and that hybrid SiO_2-saturated melts formed with participation of REE-depleted substrate [9]. This could promote adding of extra LILE into magma. It looks like magma contamination by metasedimentary sediments resulted in additional carbonation and further liquid immiscibility of salted carbonate melt. Similar to model systems [15-17], during formation of Matcha pluton, conjugated silicate liquid with syenite composition retains predominantly Nb, Ta, Zr, Hf, but not REE (figure 1d). Based on experimental data, carbonate melt extract REE, Sr, Ba better when pressure and H_2O content increases. Thus, REE-depleted varieties of studied carbonatites could have been formed at a later stage of the magmatic process under conditions of decompression and degassing of the aqueous fluid.
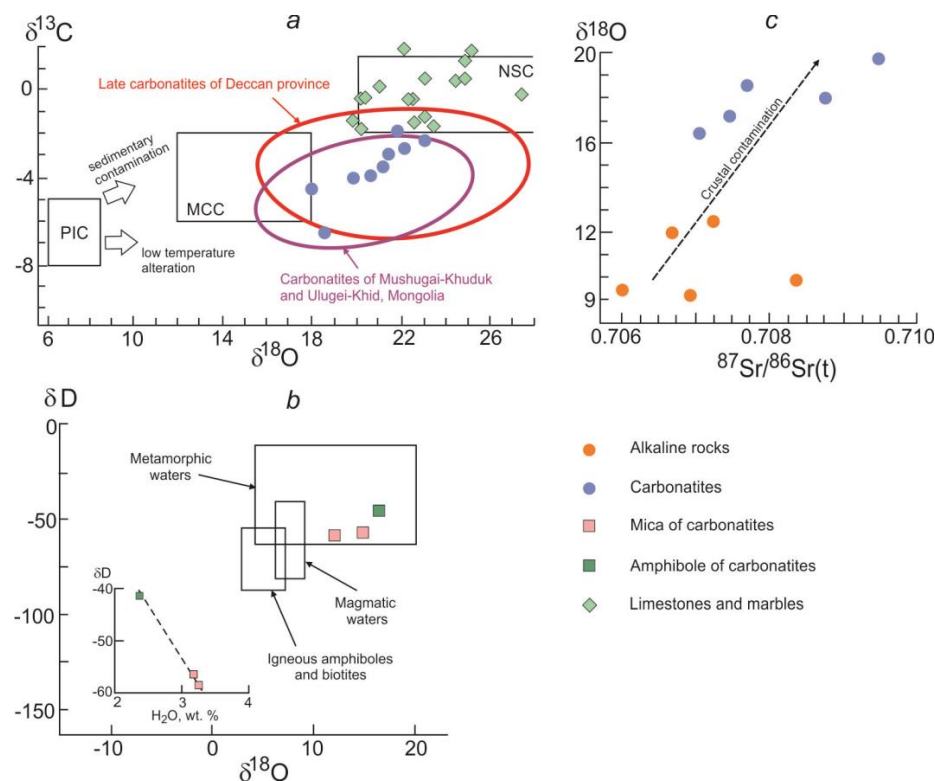

Figure 3. $\delta^{13}C$ vs. $\delta^{18}O$ (*a*), δD vs. $\delta^{18}O$ (*b*), and $^{87}Sr/^{86}Sr(t)$ vs. $\delta^{18}O$ (*c*) plots for the Matcha intrusive complex. PIC (primary igneous carbonatites) field and shifts of changes in the O-C isotopic compositions are according to (Conway and Taylor, 1969; Demény et al., 1998) [35, 36]; MCC = mantle-crustal carbonatites of the western CAOB [37]; NSC = normal sedimentary carbonates [38]. Shown for reference are: compositions of late carbonatites in the Deccan volcanic province in India and carbonatite dikes, veins, breccia and tuffs in Southern Mongolia [39, 40]; magmatic and metamorphic waters, igneous hornblende and biotite [38, 41, 42]. The data on carbonatite-alkaline magmatic complexes hosted by limestones and marbles in the western CAOB are from (Kuleshov, 1986; Doroshkevich et al., 2012; Vrublevskii et al., 2012; Vrublevskii, 2015) [5–7, 40].

Suggested magmatic nature of carbonatites from the Matcha massif is also shown as the earliest high-temperature paragenesis that includes predominant carbonates, Fe–Mg silicates, K–Na feldspars, apatite, and magnetite. In the absence of isotope reversal in the assemblage, the calculated temperatures of $\Delta^{18}O$ isotope fractionation between carbonate, magnetite, and apatite are assumed to

be equilibrium and may indicate the end of crystallization at ~400–500°C. Extraction of accessory pyrochlore from the melt is indicated by presence of chemical zoning in grains with enrichment in UO_2 and lowering of Nb, Ca, Na, and F concentrations at a late magmatic stage of carbonatite genesis [12]. Therefore, VA number of vacancies at the A site ~ 0.1–0.2 apfu in crystal-chemical formula of the mineral does not exceed values typical for igneous carbonatites [46].

4.2. Mantle-crust sources and geodynamic setting of the alkaline magmatism
Compared to younger nephelinite-carbonatite volcanism of the East African Rift produced by mixing of magmas from the HIMU and EM1 mantle reservoirs [33], Triassic alkaline intrusions of Turkestan-Altai have less radiogenic isotope composition of Nd and are enriched in ^{87}Sr (ε_{Nd}(t) ~ −11 to 0, ε_{Sr}(t) ~ 25–74). Along with primary ratios ^{207}Pb/^{206}Pb = 0.851 and ^{208}Pb/^{206}Pb = 2.089 in pyrrhotite from carbonatites, this can indicate mixing of mantle plume components PREMA-type with material of enriched lithospheric mantle EM 2 (see figure 2).

Late Paleozoic-Early Mesozoic tectonic units in the adjacent Turkestan-Alai segment are mainly composed from accretionary-collisional clastic-carbonate and volcanic rocks. Therefore, intrusions in island arc complexes may be contaminated with material bearing such geochemical signatures. In fact, distribution of the most HFSE in studied gabbro inherits spectral profile of IAB and partially OIB (see figure 1), meanwhile varieties with the most potassium content correspond to shoshonite series from ACM. Taking this into account, relative enrichment of all rocks in Cs, Rb, Ba, K, Th, U, Sr and low REE content should be considered as the result of magma contamination by crustal components. Obviously, their participation is seen in enrichment of minerals in ^{207}Pb, ^{206}Pb, ^{34}S, ^{13}C, ^{18}O and direct correlation of values δ^{18}O c δ^{13}C и ^{87}Sr/^{86}Sr(t) (see figures 2, 3). We assume that metamorphic fluid source was buried brines that possibly became mobilized upon conductive heating of carbonate sediments by intruding magma [4].

Note that many basalts in the large igneous province of the northern Tarim craton margin adjacent to the Tien Shan have similar Nd–Sr–Pb isotope compositions (see figure 2). Its formation may result from the activity of the Early Permian (~290 Ma) plume [24]. The Turkestan-Alai postorogenic alkaline magmatism possibly acted in a setting of local extension and was the final stage ("last echo") of the Tarim plume.

5. Conclusion
(1) Postorogenic plutonism in the Turkestan-Alai segment of the Kyrgyz Southern Tien Shan produced alkaline gabbro and alkaline and nepheline syenites coexisting with high-temperature liquation carbonatites. (2) The alkaline rocks and carbonatites have a parental magma source, possibly, due to mixing of PREMA and EM 2-type material. Plume-lithospheric interactions led to syntexis and hybrid melting whereby magma became contaminated with crustal material. (3) The HFSE patterns in early alkaline gabbro bear signatures of interaction between the primary mafic magma and IAB-type material. Strong isotope similarity of alkaline rocks with basalts of the Tarim large igneous province suggests that they have similar plume source.

References
[1]   Bell K, Kjarsgaard B A and Simonetti A 1998 Carbonatites – into the twenty-first century *Journal of Petrology* 39 1839–1845
[2]   Gwalani L G, Moore K and Simonetti A 2010 Carbonatites, alkaline rocks and the mantle: a special issue dedicated to Keith Bell *Mineralogy and Petrology* 98 5–10

[3]   Bell K and Simonetti A 2010 Source of parental melts to carbonatites–critical isotopic constraints *Mineralogy and Petrology* 98 77–89

[4]   Pokrovskii B G, Andreeva E D, Vrublevskii V V and Grinev O M 1998 Contamination mechanisms of alkaline-gabbro intrusions in the southern periphery of the Siberian craton: evidence from strontium and oxygen isotopic compositions *Petrologiya* 6 237–251

[5]   Doroshkevich A G, Ripp G S, Izbrodin I A and Savatenkov V M 2012 Alkaline magmatism of the Vitim province, West Transbaikalia, Russia: Age, mineralogical, geochemical and isotope (O, C, D, Sr and Nd) data *Lithos*, 152 157–172

[6]   Vrublevskii V V, Krupchatnikov V I, Izokh A E and Gertner I F 2012 The alkaline and carbonatitic rocks of Gorny Altai (Edel'veis complex) as indicators of Early Paleozoic plume magmatism in the Central Asian Fold Belt *Russian Geology and Geophysics* 53 721–735

[7]   Vrublevskii V V 2015 Sources and geodynamic setting of petrogenesis of the Middle Cambrian Upper Petropavlovka alkaline basic pluton (Kuznetsk Alatau, Siberia) *Russian Geology and Geophysics* 56 379–401

[8]   Shinkarev N F 1978 *Origin of Igneous Rocks* (Leningrad: Nedra) p 304 (in Russian)

[9]   Nenahov V M 2002 *Late Paleozoic collisional magmatism and metallogeny of the Turkestan-Alai. Metallogeny of Collisional Geodynamic Settings* (Book 2) ed N V Mezelovskii (Moscow: GEOS) pp. 125–220 (in Russian)

[10]   Solomovich L I 2007 Postcollisional magmatism in the South Tien Shan Variscan Orogenic Belt, Kyrgyzstan: Evidence for high-temperature and high-pressure collision *Journal of Asian Earth Sciences* 30 142–153

[11]   Mayorov I P and Gavrilin R D 1971 Carbonatites of the Late Palaeozoic Turkestan-Alai geosynclines *Sovetskaya Geologiya* 10 111–116

[12]   Vrublevskii V V, Bukharova O V and Morova A A 2016 The Nb-Ti mineralization of calcite-dolomite carbonatites of the Matcha alkaline pluton, Alay Range, Southern Tien Shan. *Geosfernye Issledovaniya* 1 52–65

[13]   Sun S. and McDonough W F 1989 Chemical and isotopic systematics of oceanic basalts: implications for mantle composition and processes *Geol. Soc. Spec. Publ.*, 42 313–345

[14]   Kelemen P B, Hanghøj K and Greene A R 2003 One view of the geochemistry of subduction-related magmatic arcs, with an emphasis on primitive andesite and lower crust Treatise on *Geochemistry* Elsevier Ltd. 3 pp 593–659

[15]   Martin L H J, Schmidt M W, Mattsson H B and Guenther D 2013 Element partitioning between immiscible carbonatite and silicate melts for dry and H2O-bearing systems at 1–3GPa *Journal of Petrology* 54 2301–2338

[16]   Jones J H, Walker D, Pickett D A, Murell M T and Beattie P 1995 Experimental investigations of the partitioning of Nb, Mo, Ba, Ce, Pb, Ra, Th, Pa, and U between immiscible carbonate and silicate liquids *Geochimica et Cosmochimica Acta* 59 1307–1320

[17]   Veksler I V, Petibon C, Jenner G A, Dorfman A M and Dingwell D B 1998 Trace element partitioning in immiscible silicate-carbonate liquid systems: an initial experimental study using a centrifuge autoclave *Journal of Petrology* 39 2095–2104

[18]   Guzmics T, Zajacz Z, Mitchell R H, Szabó C and Wälle M 2015 The role of liquid-liquid immiscibility and crystal fractionation in the genesis of carbonatite magmas: insights from Kerimasi melt inclusions *Contributions to Mineralogy and Petrology* 169 article 17

[19]   Vladykin N V, Morikiyo T, and Miyazaki T 2005 Sr and Nd isotopes geochemistry of alkaline and carbonatite complexes of Siberia and Mongolia and some geodynamic implications Sources of Deep Magmatism and Plumes Irkutsk 19–37

[20]   Vrublevskii V V and Gertner I F 2005 Origin of carbonatite-bearing complexes from fold systems: isotopic evidence for the mantle-crust interaction Sources of Deep Magmatism and Plumes Irkutsk 38–58

[21]   Nikiforov A V, Yarmolyuk V V, Kovalenko V I, Ivanov V G and Zhuravlev D Z 2002 Late Mesozoic carbonatites of western Transbaikalia: Isotopic–geochemical characteristics and

        sources *Petrologiya* 10 146–164

[22] Xu C, Taylor R N, Kynicky J, Chakhmouradian A R, Song W and Wang L 2011 The origin of enriched mantle beneath North China block: evidence from young carbonatites *Lithos* 127 1–9

[23] Vrublevskii V V, Voitenko N N, Romanov A P, Polyakov G V, Izokh A E, Gertner I F and Krupchatnikov V I 2005 Magma sources of Triassic lamproites of Gornyi Altai and Taimyr: Sr and Nd isotope evidence for plume–lithosphere interaction *Doklady Earth Sciences* 405A 1365–1367

[24] Zhang Y, Liu J and Guo Z 2010 Permian basaltic rocks in the Tarim basin, NW China: implications for plume–lithosphere interaction *Gondwana Research* 18 596–610

[25] Li Y Q, Li Z L, Sun Y L, Santosh M, Langmuir C H, Chen H L, Yang S F, Chen Z X and Yu X 2012 Platinum-group elements and geochemical characteristics of the Permian continental flood basalts in the Tarim Basin, northwest China: Implications for the evolution of the Tarim Large Igneous Province *Chemical Geology* 328 278–289

[26] Wei X, Xu Y G, Feng Y X and Zhao J X 2014 Plume-lithosphere interaction in the generation of the Tarim large igneous province, NW China: geochronological and geochemical constraints *American Journal of Science* 314 314–356

[27] Zindler A and Hart S R 1986 Chemical geodynamics Ann. Rev. Earth Planet. Sci., 14 493–571

[28] Stracke A, Hofmann A W and Hart S R 2005 FOZO, HIMU, and rest of the mantle zoo *Geochemistry, geophysics, geosystems* 6 1–20.

[29] Stacey J C and Kramers J D 1975 Approximation of terrestrial lead isotope evolution by a two-stage model *Earth and Planetary Science Letters* 26 207–221

[30] Zartman R E and Doe B R 1981 Plumbotectonics – the model *Tectonophysics* 75 135–162

[31] Hart S R, Hauri E H, Oschmann L A and Whitehead J A 1992 Mantle plumes and entrainment: isotopic evidence Science 256 517–520

[32] Armienti P and Gasperini D 2007 Do we really need mantle components to define mantle composition? *Journal of Petrology* 48 693–709

[33] Bell K and Tilton G R 2001 Nd, Pb and Sr isotopic compositions of East African carbonatites: evidence for mantle mixing and plume inhomogeneity *Journal of Petrology* 42 1927–1945

[34] Vrublevskii V V, Krupchatnikov V I and Gertner I F 2017 The role of mantle in the development of Early Paleozoic oceanic islands volcanism (for the geochemical data of OIB from SE Altai Mountains) *Geosfernye Issledovaniya* 1 28–38

[35] Conway C H and Taylor H P 1969 18O/16O and 13C/12C ratios of coexisting minerals in the Oka and Magnet Cove carbonatite bodies *Journal of Geology* 77 618–626

[36] Demény A, Ahijado A, Casillas R and Vennemann T W 1998 Crustal contamination and fluid/rock interaction in the carbonatites of Fuerteventura (Canary Islands, Spain): a C, O, H isotope study *Lithos* 44 101–115

[37] Vrublevskii V V 2017 Typical δ13C–δ18O ratios in mantle-crustal carbonatites of the CAOB Abstr. 27 th Goldschmidt conference Paris

[38] Pokrovskii B G 2000 Crustal Contamination of Mantle Magmas: Evidence from Isotope Geochemistry (Moscow: Nauka) p 228. (in Russian)

[39] Ray J S, Ramesh R, Pande K, Trivedi J R, Shukla P N and Pate P.P. 2000 Isotope and rare earth element chemistry of carbonatite-alkaline complexes of Deccan volcanic province: implications to magmatic and alteration processes *Journal of Asian Earth Sciences* 18 177–194

[40] Kuleshov V N 1986 Isotopic composition and origin of deep carbonates (Moscow: Nauka) p 124 (in Russian)

[41] Sheppard S M F 1986 Characterization and isotopic variations in natural waters *Reviews in Mineralogy* 16 165–184

[42] Taylor H P Jr and Sheppard S M F 1986 Stable isotopes in high temperature geological processes *Reviews in Mineralogy* 16 227–269

[43] Clayton R N and Kieffer S W 1991 Oxygen isotopic thermometer calibrations *The Geochem. Soc. Spec. Publ.*, 3 3–10

[44] Fortier S M and Luttge A 1995 An experimental calibration of the temperature dependence of oxygen isotope fractionation between apatite and calcite at high temperatures (350–800oC) *Chemical Geology* 125 281–290

[45] Alberti A, Castorina F, Censi P, Comin-Chiaramonti P and Gomes C B 1999 Geochemical characteristics of cretaceous carbonatites from Angola *Journal of African Earth Sciences* 29 735–759

[46] Nasraoui M and Bilal E 2000 Pyrochlores from the Lueshe carbonatite complex (Democratic Republic of Congo): a geochemical record of different alteration stages *Journal of Asian Earth Sciences* 18 237–251